

**Black Holes in Cascading Theories:
Confinement/Deconfinement Transition
and other Thermal Properties**

Manavendra Mahato¹, Leopoldo A. Pando Zayas¹
and César A. Terrero-Escalante²

¹ *Michigan Center for Theoretical Physics
Randall Laboratory of Physics, The University of Michigan
Ann Arbor, MI 48109-1120, USA*

² *Departamento de Física Teórica, Instituto de Física
Universidade do Estado do Rio de Janeiro
Maracanã, 20559-900 RJ, Brazil*

Abstract

We present numerical evidence for a transition between the Klebanov-Strassler background and a solution describing a black hole in the class of cascading solutions in the chirally restored phase. We also present a number of properties of this solution, including the running of the coupling constant, the viscosity to entropy ratio and the drag force on a quark moving in this background.

1 Introduction

The AdS/CFT correspondence provides an alternative way to study the strongly coupled regime of gauge theories via gravity duals. The original statement of the AdS/CFT correspondence identifies $\mathcal{N} = 4$ supersymmetric Yang-Mills with IIB string theory on $AdS_5 \times S^5$ [1, 2]. At finite temperature the gravity side is described by nonextremal D3 branes and the qualitative matching of the properties was one of the key observations in the understanding and eventual formulation of the AdS/CFT correspondence [3]. Other interesting aspects of finite temperature theories, as seen by the AdS/CFT correspondence were discussed by Witten [4]. In particular, the Hawking-Page phase transition in the gravity side was related to the confinement/deconfinement transition on the field theory side.

In a remarkable series of papers [5, 6, 7, 8, 9] Klebanov and collaborators carried out a program that concluded with a supergravity background that is dual to a confining field theory with chiral symmetry breaking. This background is known as the warped deformed conifold or the Klebanov-Strassler (KS) solution. In the context of the gauge/gravity correspondence it is natural to ask about the possible deconfinement transition for the dual field theory at finite temperature. The finite temperature phase of such theory is certainly very interesting and has been tackled in various papers including [11, 12, 13]. In particular, reference [13] constructed a perturbative solution whose regime of validity is restricted to high temperature and small value of the F_3 flux: $\int_{\Sigma_3} F_3 = P$. Further improvements to this solution were presented in [14]. Knowing the solution only asymptotically in the radial coordinate and for a specific regime of parameters prevents us from extracting the full thermodynamics and from being able to understand possible phase transitions. In particular, to answer questions that require knowing the solution for all values of the radial coordinate, like question involving the action, it is important to have the full solution which was found numerically in [15].

The thermodynamic aspects of strongly coupled field theories have gained a lot of attention recently, largely stimulated by RHIC. Some of the thermodynamic aspects discussed in this paper for similar models have been considered in simpler supergravity backgrounds in [19, 20, 21, 22, 23]. The literature is by now very extensive, a representative sample of the different questions that are being pursued can be found in the pages of the Perimeter Institute, where part of our results were preliminarily presented [24].

The paper is organized as follows. We review the construction of the cascading

black hole in section 2. In section 3 we start by briefly reviewing the KS solution including a convenient one-dimensional presentation. Then we present our main result which is the transition between the KS solution and the cascading black hole. Section 4 discusses various properties of the cascading black hole, including the running of the coupling constant at finite temperature, comments on the viscosity bound and the drag force. We conclude in section 5 with a brief discussion of our main results and some open questions.

2 Review of the cascading black hole

To understand the Ansatz for the finite temperature solution we start from the conformal case where the supergravity background is $AdS_5 \times T^{1,1}$ and the field theory was discussed in [5]. The five dimensional manifold denoted by $T^{1,1}$ is parametrized by coordinates $(\psi, \theta_1, \phi_1, \theta_2, \phi_2)$. The construction of the Ansatz follows directly the one presented originally in [12]. For the metric we consider a generalization consistent with the $U(1)$ symmetry generated by ψ -rotations¹. The Ansatz in question depends on four functions (x, y, z, w) of the radial coordinate denoted by u :

$$ds^2 = e^{2z}(-e^{-6x}dX_0^2 + e^{2x}dX_i dX^i) + e^{-2z}ds_6^2, \quad (2.1)$$

where

$$\begin{aligned} ds_6^2 &= e^{10y}du^2 + e^{2y}(dM_5)^2, \\ (dM_5)^2 &= e^{-8w}e_\psi^2 + e^{2w}(e_{\theta_1}^2 + e_{\phi_1}^2 + e_{\theta_2}^2 + e_{\phi_2}^2) \equiv e^{2w}ds_5^2. \end{aligned} \quad (2.2)$$

The Funfbein is:

$$e_\psi = \frac{1}{3}(d\psi + \cos\theta_1 d\phi_1 + \cos\theta_2 d\phi_2), \quad e_{\theta_i} = \frac{1}{\sqrt{6}}d\theta_i, \quad e_{\phi_i} = \frac{1}{\sqrt{6}}\sin\theta_i d\phi_i. \quad (2.3)$$

The qualitative meaning of the metric functions x, y, w and z was explained in [12, 15].

The Ansatz for the p -form fields is as in the original Klebanov-Tseytlin (KT) solution [8]:

¹In the gauge theory [5] this symmetry is identified with the $U(1)_R$. Restoring this symmetry at high temperature is understood as chiral symmetry restoration [13]. Therefore, the solution we constructed in [15] corresponds to the deconfined phase due to the presence of a horizon but also to the phase with the chiral symmetry restored due to the fact that $U(1)_\psi$ is a symmetry of the background.

$$\begin{aligned}
F_3 &= P e_\psi \wedge (e_{\theta_1} \wedge e_{\phi_1} - e_{\theta_2} \wedge e_{\phi_2}) , \\
B_2 &= f(u)(e_{\theta_1} \wedge e_{\phi_1} - e_{\theta_2} \wedge e_{\phi_2}) , \\
F_5 &= \mathcal{F} + *\mathcal{F} , \quad \mathcal{F} = K(u) e_\psi \wedge e_{\theta_1} \wedge e_{\phi_1} \wedge e_{\theta_2} \wedge e_{\phi_2} .
\end{aligned} \tag{2.4}$$

Note that the form of F_3 is such that it describes a constant flux along a 3-cycle, that is, $\int_{\Sigma_3} F_3 = P$. In some other notation this is called the number of fractional D3 branes. The Bianchi identity for the 5-form, $d * F_5 = dF_5 = H_3 \wedge F_3$, implies

$$K(u) = Q + 2P f(u) , \tag{2.5}$$

where Q is a constant. P and Q are known as M and N in the standard literature (see review [10]).

Thus, in the presence of 3-form flux ($P \neq 0$), the flux of F_5 varies with the radius. The fact that $K(u)$ depends on the coordinate u is very novel and has interesting physical implications. Phenomenologically, a very attractive property of this class of supergravity solutions is that it encodes the logarithmic running of a combination of gauge couplings in field theory. It does so via a varying B_2 field which is compensated by a constant F_3 flux through a 3-cycle. The five-form, which is constant in most solutions, varies according to the Bianchi identity $dF_5 = H_3 \wedge F_3$ and generates a varying flux as $\int_{\Sigma_5} F_5$ depends on the radial coordinate. The supergravity solution therefore has varying flux. This varying flux was interpreted in [9] as the dual of a Seiberg duality cascade, coining therefore the term of cascading solutions.

2.1 The system of equations from reduction to 1-d

An efficient way to derive the system of type IIB supergravity equations of motion is to start with the 1-d effective action for the radial evolution which follows from the 10-d action. This approach is convenient because to establish the transition we compare the actions. So, a simple action is an advantage.

The type IIB supergravity equations of motion follow from the action

$$\begin{aligned}
S_{10} = & -\frac{1}{2\kappa_{10}^2} \int d^{10}x \left(\sqrt{-g_{10}} \left[R_{10} - \frac{1}{2}(\partial\Phi)^2 - \frac{1}{12}e^{-\Phi}(\partial B_2)^2 \right. \right. \\
& \left. \left. - \frac{1}{2}e^{2\Phi}(\partial\mathcal{C})^2 - \frac{1}{12}e^\Phi(\partial\mathcal{C}_2 - \mathcal{C}\partial B_2)^2 - \frac{1}{4\cdot 5!}F_5^2 \right] \frac{1}{-2\cdot 4!\cdot (3!)^2} \epsilon_{10} C_4 \partial C_2 \partial - B_2 + \dots \right) , \tag{2.6}
\end{aligned}$$

$$(\partial B_2)_{\dots} = 3\partial_{[.} B_{.]}, \quad (\partial C_4)_{\dots} \equiv 5\partial_{[.} C_{\dots]}, \quad F_5 = \partial C_4 + 5(B_2 \partial C_2 - C_2 \partial B_2),$$

supplemented with the on-shell constrain $F_5 = *F_5$.

For the metric (2.1)

$$\sqrt{G} = \frac{1}{108} e^{10y-2z} \sin \theta_1 \sin \theta_2,$$

$$\int d^{10}x \sqrt{G} R \rightarrow C_{b.h.} \frac{1}{27} \int du [5y'^2 - 3x'^2 - 2z'^2 - 5w'^2 + e^{8y}(6e^{-2w} - e^{-12w})], \quad (2.7)$$

where $C_{b.h.} = 64 \pi^3 \beta_{b.h.} V_3$. The inverse temperature of the black hole is represented by $\beta_{b.h.}$ and V_3 is the spatial volume in the x^1, x^2 and x^3 directions.

The matter part is

$$\int d^{10}x \sqrt{G} \left[-\frac{1}{2} (\partial \Phi)^2 + \dots \right] \rightarrow -C_{b.h.} \frac{1}{27} \int du \frac{1}{8} \left[\Phi'^2 + 2e^{-\Phi+4z-4y-4w} f'^2 + 2e^{\Phi+4z+4y+4w} P^2 + e^{8z} (Q + 2Pf)^2 \right]. \quad (2.8)$$

The 1-d effective lagrangian is:

$$L = T - V,$$

$$T = 5y'^2 - 3x'^2 - 2z'^2 - 5w'^2 - \frac{1}{8} \Phi'^2 - \frac{1}{4} e^{-\Phi+4z-4y-4w} f'^2, \quad (2.9)$$

$$V = -e^{8y}(6e^{-2w} - e^{-12w}) + \frac{1}{4} e^{\Phi+4z+4y+4w} P^2 + \frac{1}{8} e^{8z} (Q + 2Pf)^2, \quad (2.10)$$

supplemented with the “zero-energy” constraint $T + V = 0$.

This is effectively a classical mechanical system. The simplest equation is for the nonextremality function x (note that it breaks Lorentz invariance in the (X^0, X^1, X^2, X^3) plane):

$$x'' = 0, \quad x = au, \quad a = \text{const.} \quad (2.11)$$

The reason for such a simple equation is that, as explained in [12], it does not appear in the effective one dimensional Lagrangian, except for its kinetic term.

The other functions y, w, z, f and Φ should satisfy a coupled system of equations:

$$\begin{aligned} 10y'' - 8e^{8y}(6e^{-2w} - e^{-12w}) + \Phi'' &= 0, \\ 10w'' - 12e^{8y}(e^{-2w} - e^{-12w}) - \Phi'' &= 0, \\ \Phi'' + e^{-\Phi+4z-4y-4w} (f'^2 - e^{2\Phi+8y+8w} P^2) &= 0, \\ 4z'' - (Q + 2Pf)^2 e^{8z} - e^{-\Phi+4z-4y-4w} (f'^2 + e^{2\Phi+8y+8w} P^2) &= 0, \\ (e^{-\Phi+4z-4y-4w} f')' - P(Q + 2Pf)e^{8z} &= 0. \end{aligned} \quad (2.12)$$

The solutions to this system are subject to the zero-energy constrain $T + V = 0$, i.e.

$$\begin{aligned} & 5y'^2 - 2z'^2 - 5w'^2 - \frac{1}{8}\Phi'^2 - \frac{1}{4}e^{-\Phi+4z-4y-4w}f'^2 - e^{8y}(6e^{-2w} - e^{-12w}) \\ & + \frac{1}{4}e^{\Phi+4z+4y+4w}P^2 + \frac{1}{8}e^{8z}(Q + 2Pf)^2 - 3a^2 = 0 . \end{aligned} \quad (2.13)$$

This constrain was used in [15] as a criterion for quality of the numerical solution and it was established that for various known solutions it was of the order 10^{-16} where the reliable accuracy was shown to be 10^{-10} (see fig.1 and section 2.3 for a detailed description).

The function y amounts to a choice of the radial coordinate. This is relevant for understanding the dimensions of all quantities. Note that in particular, the system (2.12) and the constrain (2.13) are invariant under $e^y \rightarrow L_0 e^y$ and $u \rightarrow L_0^{-4}u$ if we assume that $Q \rightarrow L_0^4 Q, P \rightarrow L_0^2 P, a \rightarrow L_0^4 a$ and $f \rightarrow L_0^2 f$. We therefore express all dimensionfull quantities in units where $L_0 = 1$.

Standard regular non-extremal D3-brane solution: To develop our intuition, we present the nonextremal D3 brane of the system (2.12) in the radial u -coordinate. It takes the following form:

$$e^{4y} = \frac{a}{\sinh 4au} , \quad e^{4z} = \frac{a}{q \sinh 4au} , \quad e^{4x} = e^{4au} . \quad (2.14)$$

Note that near the horizon ($u \rightarrow \infty$)

$$y = y_* - au + \frac{1}{4}e^{-8au} + O(e^{-16au}) , \quad z = z_* - au + \frac{1}{4}e^{-8au} + O(e^{-16au}) , \quad (2.15)$$

$$y_* = \frac{1}{4} \ln 2a , \quad z_* = \frac{1}{4} \ln \frac{2a}{q} , \quad (2.16)$$

A more recognizable form of this solution is given by:

$$ds^2 = h^{-1/2}(gdX_0^2 + dX_i dX_i) + h^{1/2}[g^{-1}d\rho^2 + \rho^2(dM_5)^2] , \quad (2.17)$$

$$g = e^{-8x} = 1 - \frac{2a}{\rho^4} , \quad \rho^4 = \frac{2a}{1 - e^{-8au}} , \quad h = e^{-4z-4x} = \frac{q}{\rho^4} . \quad (2.18)$$

Let us clarify the relationship between the radial coordinate u and the more standard coordinate ρ . Using $2a = \rho_0^4$, we have

$$du = \frac{d\rho}{\rho^5} \left(1 - \frac{\rho_0^4}{\rho^4} \right)^{-1} . \quad (2.19)$$

This can be integrated to

$$u = -\frac{1}{4\rho_0^4} \ln \left(1 - \frac{\rho_0^4}{\rho^4} \right) . \quad (2.20)$$

Note that in the domain of $\rho_0 \leq \rho < \infty$ we have that u ranges in $0 < u < \infty$. For large values of ρ we have that $u \approx 1/4\rho^4$. The position of the horizon which is finite in the ρ coordinate becomes infinite in the u coordinates.

2.2 Universality of regular nonextremal D3 brane horizons

For the general solution of the system (2.12), in the u -coordinates the area of a surface defined by a horizon at $u = \text{constant}$ is

$$A = V\omega_5 \exp(-2z + 3x + 5y). \quad (2.21)$$

Given that the equation of motion for x has the general solution $x = au$ we are forced into the following situation. If the horizon is at $u \rightarrow \infty$, as is the case for the non-extremal D3 brane solution, then for the area A to be finite we need the following asymptotics for z and y :

$$z \rightarrow \alpha au + z_*, \quad y \rightarrow \beta au + y_*, \quad (2.22)$$

with the condition that

$$3 - 2\alpha + 5\beta = 0. \quad (2.23)$$

Note that the regular nonextremal D3 brane corresponds to $\alpha = \beta = -1$. The main claim is that: *The existence of a regular horizon fixes the asymptotic behavior of the metric coordinates x, y and z near the horizon.* Eq.(2.23) was used in [15] as a criterion of quality of the numerical solution near the horizon (see table 1 for the precision of this criterion for the solutions we discuss here).

Similarly, one can obtain an expression for the temperature. Namely, the relevant part of the metric is

$$ds^2 = e^{2z-6x} d\tau^2 + e^{-2z+10y} du^2. \quad (2.24)$$

We introduce a new radial coordinate as:

$$\rho = e^{z-3x}. \quad (2.25)$$

We can now rewrite the metric as:

$$ds^2 = \frac{e^{-4z+10y+6x}}{(z' - 3x')^2} \left[d\rho^2 + \rho^2 (e^{2z-5y-3x} (z' - 3a) d\tau)^2 \right]. \quad (2.26)$$

Note that, again, *the requirement of finite temperature fixes the large- u asymptotic of various metric functions to be $2z - 5y - 3x \rightarrow \text{constant}$* . Requiring the absence of conical singularity we find that the temperature defined as the inverse of the period is

$$T = \frac{|\alpha - 3|}{2\pi} a e^{2z_* - 5y_*}, \quad (2.27)$$

where we used that near the horizon the asymptotic form of z and y is given by (2.22).

2.3 Numerics

In Ref.[15] we gave a detailed description of the construction of solutions to the system (2.12) which contain regular black holes in the infrared (large values of u) and a cascading behavior in the ultraviolet (small values of u). We will summarize here our approach. For more details on the numerical method and the understanding of the numerical output, we refer the interested reader to Ref.[15].

To solve the equations for the metric functions we use the seventh-eight order continuous Runge-Kutta method. Thanks to its adaptive scheme, this method provides a great control upon the output accuracy. We tested and fitted the numerical procedure using a number of known analytical solutions, some of them with fixed values of the parameters (for instance, the non-extremal D3 black hole, with $P = 0$, and the KT background, with $a = 0$). Analyzing the sensitivity of the solutions to the variation of these parameters, we found that for a method tolerance of 10^{-14} , an error of 10^{-10} can be safely regarded to be negligible, what allowed us to set our numerical ‘zero’ to this last value.

Using the non-extremal D3 solution ($P = 0$), we set the boundary conditions for our ten variables at the value of u corresponding to the 90% of the distance to the horizon. A correction is introduced to enforce the solution with $P \neq 0$ to satisfy constrain (2.13) in this boundary.

Next we integrate backward and, for a given value of a and Q , we find the value of P such that the space is complete, i.e., $u_{sing} \approx 0$ (see section 2.4 and table 1). We use

$$f_1 + P e^{\Phi_0 + 4y_0 + 4w_0} = 0, \quad (2.28)$$

to check that this singularity is of the type given by

$$z = -\frac{1}{4} \ln [4(u - u_{sing})], \quad (2.29)$$

a	P	$u_{90\%}$	$3 - 2\alpha + 5\beta$	u_{sing}	$f_1 + Pe^{\phi_0+4y_0+4w_0}$
1	4.26906025	2.19361453	-9×10^{-15}	3×10^{-10}	0.00001257
0.5	2.87343889	4.387229	-7×10^{-15}	3×10^{-11}	0.0000065
0.1	1.094389139	21.9361453	-2×10^{-15}	4×10^{-10}	0.00000002
0.01	0.316430028	219.361453	10^{-15}	2×10^{-9}	0.0000000002

Table 1: Values of the parameters used for the four cases presented in this manuscript. $Q = L_p = 1$ was used everywhere.

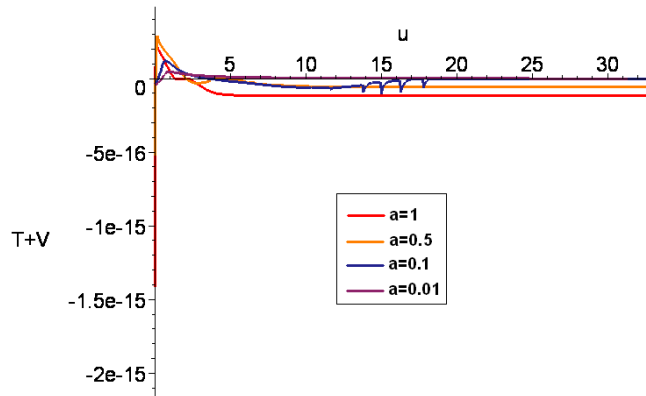


Figure 1: The Hamiltonian constrain for the cases in table 1.

and that the remaining fields are analytical at u_{sing} . In this criterion, the subindices indicates that these are coefficients in Taylor series for the corresponding field at u_{sing} .

We then integrate the system forward and identify numerically the presence of a horizon. One of the criteria used is that given by Eq.(2.23).

In table 1 we present the values of the parameters and the results for the infrared and ultraviolet criteria of quality for four cases that are going to be used as examples throughout this manuscript.

We also recall that system (2.12) was modified in such a way that the solutions must automatically satisfy constrain (2.13). This allows to use the constrain as a dynamical criterion of the quality of the numerical output for any value of the parameters. Indeed, all our solutions are warranted to satisfy constrain (2.13) within the accuracy given by our numerical ‘zero’. This can be verified in fig.1. For all the four cases in the table, the $T + V = 0$ constrain is satisfied in the whole range of the radial coordinate.

2.4 UV asymptotics and completeness of the solution

Let us first discuss the completeness of our solution. The statement that completeness of the space requires $u_{sing} = 0$ was made explicitly in [15] (see section 4.2 there), however, the details were not shown. Here we provide those details since they are crucial in clarifying the number of parameters of the solution².

The asymptotic form of the relevant part of the metric, as obtained in [15], is given for $z(u)$ by Eq.(2.29) and for $y(u)$ by $\exp(4y) = 1/4u$. The first expression was widely discussed in [15] and we refer the reader to that paper for details, including the fittings. The expression of y is ubiquitous in the region of small values of u . It is valid in the asymptotic region for all the solutions we know: KW [5], nonextremal D3 branes [12], KT [8] and KS [9]. The best fit analysis presented in [15] indicates that this seems to be also the case for our numerical solution.

To discuss completeness we consider an outgoing null geodesic toward the asymptotic regions of small u . The corresponding effective Lagrangian is:

$$\mathcal{L} = -e^{2z-6x} \dot{t}^2 + e^{-2z+10y} \dot{u}^2. \quad (2.30)$$

With this information the affine time for a geodesic to reach u_{sing} satisfies:

$$d\lambda = \frac{1}{E} u^{-5/4} du. \quad (2.31)$$

Note that this is independent of the precise form of the z function in the metric. The structure of the function z enters only through the integration limits. Namely, the above equation can be integrated to yield

$$\lambda = \frac{4}{E} \left(\frac{1}{u_{sing}} - \frac{1}{u_{in}} \right). \quad (2.32)$$

Here u_{in} should be viewed as a cutoff, beyond this point we do not know the precise formula for y , however, we assume that this geodesic originates somewhere near the black hole horizon. Note that the value u_{sing} enters just through the integration limits, since the full solution does not exist for $u < u_{sing}$. As can be seen from (2.32) the affine parameter is infinite only for $u_{sing} = 0$. We need an infinite affine parameter to guarantee completeness of the solution. Thus, *the solution is complete only for $u_{sing} = 0$.*

²This point has been an important source of discussion with A. Buchel and we hope that this section clarifies that $u_{sing} = 0$ fixes one of the three seemingly free parameters (Q, P, a) .

The number of relevant parameters

Thus, superficially, our solutions depend on three parameters, a , P and Q . However, the condition $u_{sing}(\dots; a, P, Q) = 0$ imposes a new constrain on the solutions that effectively reduces the number of parameters to two.

For instance, fixing $Q = 1$, for the values of a given in table 1, it is found that the expression,

$$u_{sing} = be^{-P^2} + b_0 + b_1P + b_2P^2 + \dots, \quad (2.33)$$

fits very well the numerical output. Note that the first term is clearly related to the strong energy scale as indicated by the KT formula, that is, it is related to the radial position where the KT warp factor vanishes; of course, there are many corrections as the KT warp factor is not the full answer. To illustrate the origins and robustness of the expression (2.33), let us first discuss a specific point in the graph 2 to highlight the importance of the first term in the above expansion. Namely, for $a = 0.5$, a fit to the value of u_{sing} without the exponential term (i.e., setting $b=0$) yields the following result for the coefficients b_i :

$$\{0.05854539, -0.25108172, 0.14454983, -0.03078276, \\ 0.00347435, -0.00020362, 0.488 \times 10^{-5}\},$$

with a goodness on the order of 10^{-7} . It is important to stress that for each term we verify that $b_i \leq b_{i+1}$, which indicates convergence. Now, introducing the exponential term, the result is $b = 5.49169633$,

$$\{-0.09506874, -0.09298412, 0.07882655, -0.01663906, \\ 0.00180981, -0.00010186, 0.234 \times 10^{-5}\},$$

with a goodness on the order of 10^{-9} . The ratio b_i/b_{i+1} is also much better behaved. In general the exponential term seems to be crucial for the form of u_{sing} . Thus, for (a, Q) fixed, by setting $u_{sing} = 0$ in expression (2.33), we are this way selecting a given value of P . A similar analysis was carried out for the other values of a in table 1 and another ten cases not included in the table but shown as crosses in fig.2. The curve in this figure represents the pairs (a, P) that guarantee u_{sing} to vanish for $Q = 1$. It was obtained as the best fit solution,

$$P = 4.26846923 a^{0.59296839} + 0.02429978$$

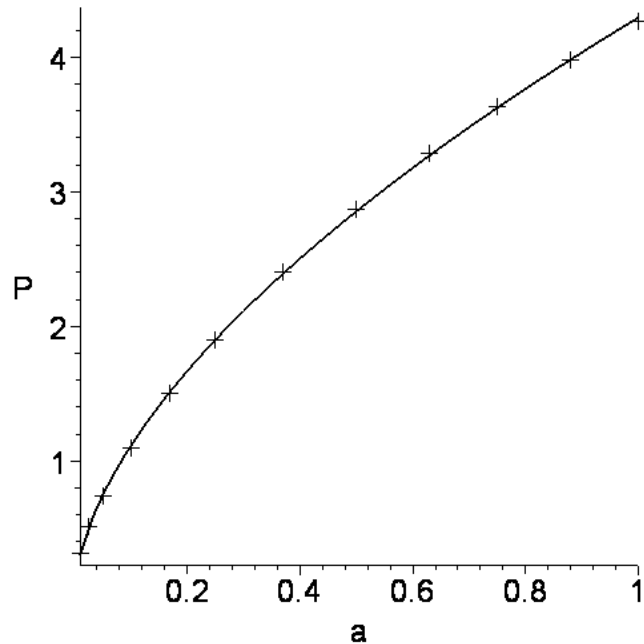


Figure 2: Values of P and a that guarantee u_{sing} to vanish for $Q = 1$.

with a goodness of 0.00124, which is satisfactory if the small amount of data used is taken into account.

Summarizing, for any values of two of the parameters determining our solution, the value of the third one is fixed by imposing completeness of the solution in the asymptotically UV region.

3 The Hawking-Page transition

There is mounting evidence for the transition we are going to describe here. In particular, similar transitions have been established in some simpler holographic models, including [29, 30].

We assume here that the confined phase is dual to the KS background. Therefore, we will first review this model and then proceed to give evidence for the transition itself.

3.1 The warped deformed conifold: Klebanov-Strassler background

The KS metric is of the form:

$$\begin{aligned}
ds_{10}^2 &= h^{-1/2}(\tau)dx_ndx_n + h^{1/2}(\tau)ds_6^2, \\
ds_6^2 &= \frac{1}{2}\varepsilon^{4/3}K(\tau)\left[\frac{1}{3K^3(\tau)}(d\tau^2 + (g^5)^2) \right. \\
&\quad \left. + \cosh^2\left(\frac{\tau}{2}\right)[(g^3)^2 + (g^4)^2] + \sinh^2\left(\frac{\tau}{2}\right)[(g^1)^2 + (g^2)^2]\right], \tag{3.1}
\end{aligned}$$

the one-forms g^i are defined as

$$\begin{aligned}
g^1 &= \frac{e^1 - e^3}{\sqrt{2}}, & g^2 &= \frac{e^2 - e^4}{\sqrt{2}}, \\
g^3 &= \frac{e^1 + e^3}{\sqrt{2}}, & g^4 &= \frac{e^2 + e^4}{\sqrt{2}}, \\
&& g^5 &= e^5, \tag{3.2}
\end{aligned}$$

where

$$\begin{aligned}
e^1 &\equiv -\sin\theta_1 d\phi_1, & e^2 &\equiv d\theta_1, \\
e^3 &\equiv \cos\psi \sin\theta_2 d\phi_2 - \sin\psi d\theta_2, \\
e^4 &\equiv \sin\psi \sin\theta_2 d\phi_2 + \cos\psi d\theta_2, \\
e^5 &\equiv d\psi + \cos\theta_1 d\phi_1 + \cos\theta_2 d\phi_2. \tag{3.3}
\end{aligned}$$

The function in the metric is

$$\mathcal{K}(\tau) = \frac{(\sinh(2\tau) - 2\tau)^{1/3}}{2^{1/3} \sinh \tau}. \tag{3.4}$$

For asymptotically large values of τ one can introduce a natural radial coordinate $r^2 = \frac{3}{2^{5/3}}\varepsilon^{4/3}e^{2\tau/3}$ such that the metric on the conifold becomes $ds_6^2 \approx dr^2 + r^2 ds_{T^{1,1}}^2$.

The matter fields are as follow:

$$\begin{aligned}
F_3 &= \frac{M\alpha'}{2} \{g^5 \wedge g^3 \wedge g^4 + d[F(\tau)(g^1 \wedge g^3 + g^2 \wedge g^4)]\} \\
&= \frac{M\alpha'}{2} \{g^5 \wedge g^3 \wedge g^4(1 - F) + g^5 \wedge g^1 \wedge g^2 F \\
&\quad + F' d\tau \wedge (g^1 \wedge g^3 + g^2 \wedge g^4)\}, \tag{3.5}
\end{aligned}$$

with $F(0) = 0$ and $F(\infty) = 1/2$, and

$$B_2 = \frac{g_s M \alpha'}{2} [f(\tau) g^1 \wedge g^2 + k(\tau) g^3 \wedge g^4] , \quad (3.6)$$

$$\begin{aligned} H_3 = dB_2 &= \frac{g_s M \alpha'}{2} \left[d\tau \wedge (f' g^1 \wedge g^2 + k' g^3 \wedge g^4) \right. \\ &\quad \left. + \frac{1}{2} (k - f) g^5 \wedge (g^1 \wedge g^3 + g^2 \wedge g^4) \right] . \end{aligned} \quad (3.7)$$

The self-dual 5-form field strength may be decomposed as $\tilde{F}_5 = \mathcal{F}_5 + \star \mathcal{F}_5$. We have

$$\mathcal{F}_5 = B_2 \wedge F_3 = \frac{g_s M^2 (\alpha')^2}{4} \ell(\tau) g^1 \wedge g^2 \wedge g^3 \wedge g^4 \wedge g^5 , \quad (3.8)$$

where

$$\ell = f(1 - F) + kF , \quad (3.9)$$

and

$$\star \mathcal{F}_5 = 4g_s M^2 (\alpha')^2 \varepsilon^{-8/3} dx^0 \wedge dx^1 \wedge dx^2 \wedge dx^3 \wedge d\tau \frac{\ell(\tau)}{K^2 h^2 \sinh^2(\tau)} . \quad (3.10)$$

$$\alpha = 4(g_s M \alpha')^2 \varepsilon^{-8/3} . \quad (3.11)$$

The solution for the functions defining the matter content is:

$$\begin{aligned} F(\tau) &= \frac{\sinh \tau - \tau}{2 \sinh \tau} , \\ f(\tau) &= \frac{\tau \coth \tau - 1}{2 \sinh \tau} (\cosh \tau - 1) , \\ k(\tau) &= \frac{\tau \coth \tau - 1}{2 \sinh \tau} (\cosh \tau + 1) , \\ \ell(\tau) &= f(1 - F) + kF = \frac{\tau \coth \tau - 1}{4 \sinh^2 \tau} (\sinh 2\tau - 2\tau) . \end{aligned} \quad (3.12)$$

The warp factor with the condition that it vanishes at infinity is

$$h(\tau) = \alpha \frac{2^{2/3}}{4} I(\tau) = (g_s M \alpha')^2 2^{2/3} \varepsilon^{-8/3} I(\tau) , \quad (3.13)$$

where

$$I(\tau) \equiv \int_{\tau}^{\infty} dx \frac{x \coth x - 1}{\sinh^2 x} (\sinh(2x) - 2x)^{1/3} . \quad (3.14)$$

Two important limits are:

$$I(\tau \rightarrow 0) \rightarrow a_0 + O(\tau^2) ; \quad (3.15)$$

$$I(\tau \rightarrow \infty) \rightarrow 3 \cdot 2^{-1/3} \left(\tau - \frac{1}{4} \right) e^{-4\tau/3}, \quad (3.16)$$

where $a_0 \approx 0.71805$. At large τ the integrand becomes

$$h \approx 3^4 2^{-4} \frac{(g_s M \alpha')^2}{r^4} \ln \left(\frac{2^{5/3}}{3} \frac{r^2}{\epsilon^{4/3}} \right), \quad (3.17)$$

where we have used that for large radius $r^2 = \frac{3}{2^{5/3}} \epsilon^{4/3} e^{2\tau/3}$:

3.2 The action for the KS model

A convenient way to look at this solution is through the prism of a one-dimensional system as discussed in [18]. Motivated by the form of the deformed conifold metric we make the following ansatz for the metric

$$ds^2 = e^{2p-x} (e^{2A} dx^\mu dx^\mu + du^2) + [e^{-6p-x} g_5^2 + e^{x+y} (g_1^2 + g_2^2) + e^{x-y} (g_3^2 + g_4^2)] . \quad (3.18)$$

The ansatz for the p-forms is:

$$H_3 = du \wedge [f'(u) g_1 \wedge g_2 + k'(u) g_3 \wedge g_4] , \quad (3.19)$$

$$F_3 = F(u) g_1 \wedge g_2 \wedge g_5 + [2P - F(u)] g_3 \wedge g_4 \wedge g_5 + F'(u) du \wedge (g_1 \wedge g_3 + g_2 \wedge g_4) , \quad (3.20)$$

$$F_5 = \mathcal{F}_5 + \mathcal{F}_5^* , \quad \mathcal{F}_5 = K(u) g_1 \wedge g_2 \wedge g_3 \wedge g_4 \wedge g_5 , \quad (3.21)$$

$$K(u) \equiv Q + k(u) F(u) + f(u) [2P - F(u)] , \quad (3.22)$$

where F, f, k are functions to be determined and P and Q are constants. We explicitly ensure that the Bianchi identities for the p-forms are satisfied automatically. The 1-d action reproducing the resulting equations of motion restricted to the above ansatz has the following general structure

$$S = c \int du e^{4A} \left[3A'^2 - \frac{1}{2} G_{ab}(\varphi) \varphi'^a \varphi'^b - V(\varphi) \right] , \quad (3.23)$$

where $c = -4 \frac{Vol_9}{2\kappa_{10}^2}$. It should be supplemented with the “zero-energy” constrain

$$3A'^2 - \frac{1}{2} G_{ab}(\varphi) \varphi'^a \varphi'^b + V(\varphi) = 0 . \quad (3.24)$$

The action (3.23) is thus a classical mechanical action for the fields A and $\varphi^a = (x, y, p, \Phi, f, k, F)$. The corresponding kinetic and potential terms in (3.23) are found to be:

$$G_{ab}(\varphi) \varphi'^a \varphi'^b = x'^2 + \frac{1}{2} y'^2 + 6p'^2 + \frac{1}{4} \left[\Phi'^2 + e^{-\Phi-2x} (e^{-2y} f'^2 + e^{2y} k'^2) + 2e^{\Phi-2x} F'^2 \right] , \quad (3.25)$$

$$\begin{aligned}
V(\varphi) &= \frac{1}{4}e^{-4p-4x} - e^{2p-2x} \cosh y + \frac{1}{4}e^{8p} \sinh^2 y \\
&+ \frac{1}{8}e^{8p} \left[\hat{a}e^{-\Phi-2x}(f-k)^2 + e^{\Phi-2x}[e^{-2y}F^2 + e^{2y}(2P-F)^2] + e^{-4x}K^2 \right], \quad (3.26)
\end{aligned}$$

where K is the combination of the independent functions f, k, F given in (3.22).

The first order equations for the independent functions $A, x, y, p, f, k, F, \Phi$ are:

$$x' = -e^{-2p-2x} - \hat{a}e^{4p-2x}K, \quad y' = e^{4p} \sinh y, \quad (3.27)$$

$$p' = \frac{1}{3}e^{4p} \cosh y - \frac{1}{6}e^{-2p-2x} + \frac{1}{6}e^{4p-2x}K, \quad (3.28)$$

$$A' = -\frac{1}{3}e^{4p} \cosh y - \frac{1}{3}e^{-2p-2x} - \frac{1}{6}e^{4p-2x}K, \quad (3.29)$$

$$f' = e^{\Phi+4p+2y}(2P-F), \quad k' = e^{\Phi+4p-2y}F, \quad F' = -\frac{1}{2}e^{-\Phi+4p}(f-k), \quad \Phi' = 0. \quad (3.30)$$

The functions that we introduced in this subsection are explicitly given in terms of the solution of the previous subsection as:

$$\begin{aligned}
e^x &= \frac{1}{4}\epsilon^{4/3}\mathcal{K} \sinh(\tau)h^{1/2}, \\
e^{2p} &= 24^{1/3}h^{-1/3}\epsilon^{-8/9}\mathcal{K}^{1/3} \sinh(\tau)^{-1/3}, \\
e^y &= \tanh\left(\frac{\tau}{2}\right).
\end{aligned}$$

We will also use explicit forms for the derivative with respect to u

$$\begin{aligned}
A' &= -\frac{1}{6}(e^{4p}(e^y + e^{-y}) + 2e^{-2p}e^{-2x} + Ke^{4p}e^{-2x}), \\
p' &= \frac{1}{6}(e^{4p}(e^y + e^{-y}) - e^{-2p}e^{-2x} + Ke^{4p}e^{-2x}), \\
y' &= e^{4p} \sinh(\ln(e^y)), \quad x' = -e^{-2p}e^{-2x} - \frac{K}{2}e^{4p}e^{-2x}, \quad \Phi = \Phi' = 0, \\
k' &= Fe^{\Phi}e^{4p}e^{-2y}, \quad f' = (2P-F)e^{\Phi}e^{4p}e^{2y}, \quad F' = -\frac{f-k}{2}e^{-\Phi}e^{4p}.
\end{aligned}$$

The expression for the action we need to evaluate is finally of the form:

$$\mathcal{L} = -\frac{4}{h}e^{2x}e^{-4p}(3A'^2 - \frac{1}{2}G_{ab} - V), \quad S_{KS} = \int d\tau \mathcal{L}. \quad (3.31)$$

3.2.1 The KS background has no regular D3 branes at the apex

As noted in [9], the KS-like Ansatz allows for general solutions having $K(u)$ with arbitrary Q in (3.22). In the more standard literature Q is identified as N . These solutions are, however, singular. Namely, near the apex of the deformed conifold (small values of τ) the warp factor takes the form:

$$h \approx \frac{Q}{\tau}. \quad (3.32)$$

An alternative way of understanding this singularity is by realizing that it corresponds to the freedom to add a homogeneous solution to the warp factor. Namely, a solution of the form

$$\frac{1}{\sqrt{g_6}} \partial_\tau \left(\sqrt{g_6} g^{\tau\tau} \partial_\tau \tilde{h} \right) = 0, \quad (3.33)$$

or

$$\tilde{h} = Q \int \frac{d\tau}{\mathcal{K}^2 \sinh^2 \tau}. \quad (3.34)$$

This last statement allows to interpret the elimination of the singularity as a statement about regular D3 branes. It is possible that, as in the interpretation for the resolved conifold of [18], this divergence signals a smearing of D3 branes along a three-dimensional subspace and therefore could also be cured, not just by turning off the charge Q , but also by localizing the branes appropriately as it was done recently in Ref.[31].

This situation presents a conceptual problem. It is natural to compare a field theory with parameters $(N, M, \epsilon \sim \Lambda_{strong})$ with a theory with $(N, M, a \sim Temperature)$. In realistic cases, the scale Λ_{strong} is dynamically generated but supergravity methods are still far from achieving that. However, for KS we have $N = 0$ and for the cascading black hole we have $u_{sing} = 0$. The comparison is really not completely clear. We deal with this point while analyzing the transition in subsection 3.3.

3.3 The transition

To accurately compute the actions we used an adaptive 3-5 Simpson's quadrature. This implies $2^{n-1}8^n$ evaluations of the Lagrangian, where n is the number of iterations needed to reach the desired precision (set here to 10^{-4}) for the integral. For the cascading black hole the Lagrangian is given in terms of the numerical solutions of system (2.12). We prioritized the output accuracy over the computational effort. This means being able to obtain the actual numerical solution of (2.12) at every point

required by the quadrature, instead of finding it by interpolating between previously calculated solutions at a given set of points. The whole computation of the cascading black hole action usually takes more than 12 hours in an ordinary desktop computer. Compared with that, estimating the action of the KS background is a quick task, since the evaluation of the corresponding Lagrangian only involves the numerical integration of (3.14) which for large τ can be accurately estimated using expression (3.17). Taking the above into account, we decided to compute the cascading black hole action for the four sets of parameters given in table 1 and compare the results with the output of the KS action as we vary ϵ .

So, we calculated the cascading black hole action as given by Eqs.(2.7) and (2.8), without considering the numerical factors common to both actions. The integration was done between $u_R = 10^{-8}$ and $u_{90\%}$. Following the order in table 1, the four results are $\{738451, 762361, 733711, 804269\}$, and their logarithms are shown in fig.4 as horizontal lines. To leading order the asymptotic values of the action are independent of a . This can be seen by directly evaluating the pieces of the action as given in (2.7) and (2.8). For example, the leading contribution from (2.7) comes from z'^2 and after the integration is proportional to $1/u_R$. Similarly, from the matter part (2.8), the leading contribution comes from the last term which is independent of a ; this term also contributes a term proportional to $1/u_R$. Note that in terms of the standard radial coordinates, this terms corresponds to R^4 where R is a UV cutoff radius. This is the typical volume divergent behavior of AdS_5 as shown in [4, 29, 30].

To compare these results with those for the KS action it is necessary for both backgrounds to have the same physical temperature. This is implemented by requiring that the physical perimeter of the temporal directions match at the point of comparison:

$$\beta_{b.h.} e^{z(u_R) - 3x(u_R)} = \beta_{KS} h^{-1/4}(\tau_R). \quad (3.35)$$

This equation allows to determine β_{KS} , since for the black hole, $\beta_{b.h.}$ is determined by the absence of conical singularities (see equation (2.27)). However, we still need a way to relate τ_R and u_R . As can be seen from various examples discussed in [12, 15], in the UV the coordinate u is related to the standard radial coordinate as $u \approx 1/4r^4$; this is also true for the nonextremal D3 brane (see equation (2.20)) as well as for the KT solution, the b-deformed conifold [12], KS and the resolved conifold [18]. The relationship between the radial coordinate τ and the standard conifold radius is

$$dr = \frac{\epsilon^{2/3}}{2^{1/6} 3^{1/2}} \frac{\sinh \tau}{(\sinh 2\tau - 2\tau)^{1/3}} d\tau. \quad (3.36)$$

In the limit of large values of r we obtain:

$$r \approx \frac{3^{1/2}}{2^{5/6}} \epsilon^{2/3} e^{\tau/3}. \quad (3.37)$$

Thus, in equation (3.35) we use that

$$\tau_R \approx \frac{1}{4} \ln(\epsilon^{-8} u_R^{-3}) - 0.954771252 + \delta\tau_R. \quad (3.38)$$

The correction $\delta\tau_R$ is required to account for the limitations of the numerical analysis to deal with actual asymptotic values. It is a function of a and ϵ and we have found it to have the approximated form,

$$\delta\tau_R = C(a)\epsilon^{1/5}. \quad (3.39)$$

Our strategy to establish the existence of the transition is as follows. We assume that the transition takes place at a value of ϵ such that $a^{-8/3}\epsilon = 1$, then we find the $C(a)$ that makes both actions equal. Following the order in table 1, $C(a) = \{-2.27, -3.264, -5.85, -9.8095\}$. We note that neither the factor $C(a)$ nor the power $1/5$ are solutions of a best fit problem but just values that give satisfactory results for all cases analyzed here. Our key observation then reduces to establish that the difference of actions changes sign appropriately around this point.

Let us address a technical issue. A problem to deal with here is the singularity in the KS background for $Q \neq 0$ (see subsection 3.2.1 for details). Fortunately, although conceptually an important point, the difference between the KS actions with and without Q are qualitatively distinguishable only in the infrared regime (see for instance figures 3). In the UV regime, the leading asymptotic behavior is governed by P and not Q .

The IR behavior is easy to understand. In this region, almost at the same value of τ , the Lagrangian with $Q = 0$ has a zero and the corresponding Lagrangian with $Q \neq 0$ has a minimum. We therefore, switch at this point from the integrand with $Q \neq 0$ to the one with $Q = 0$ as a regularization of the procedure. From the quantitative point of view, for $Q = 0$ the infrared regime gives a negative contribution to the integral which increases slowly with ϵ . Thus, for a fixed a , if for small ϵ the cascading black hole action dominates the difference of the actions, this is a reliable result because the negative contribution to the integral is negligible. On the other hand, if for large ϵ the KS action dominates, that is certainly true, because it does so in spite of the negative contribution to the integral.

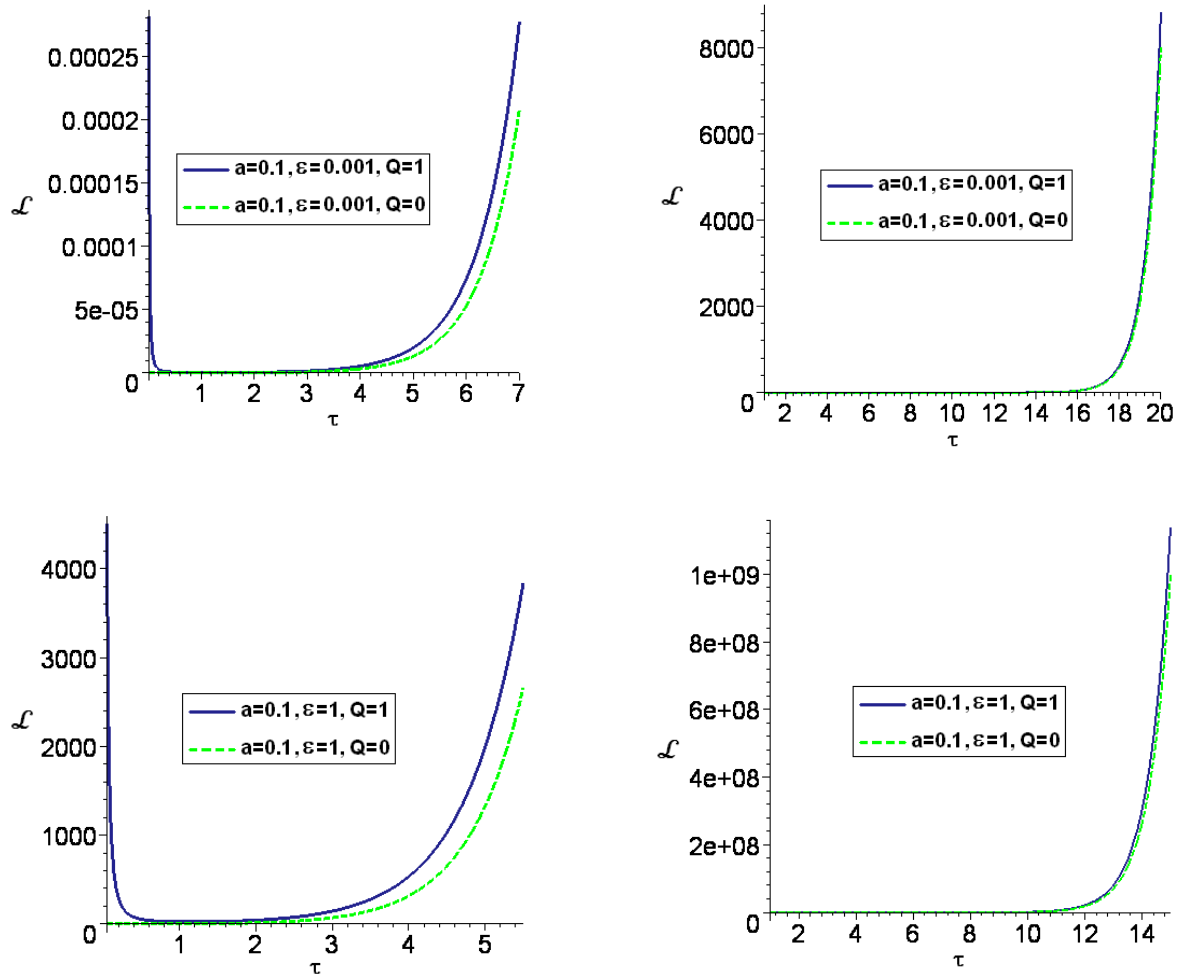


Figure 3: The KS Lagrangian in the IR and the UV for $\epsilon = 0.001$ and $\epsilon = 1$

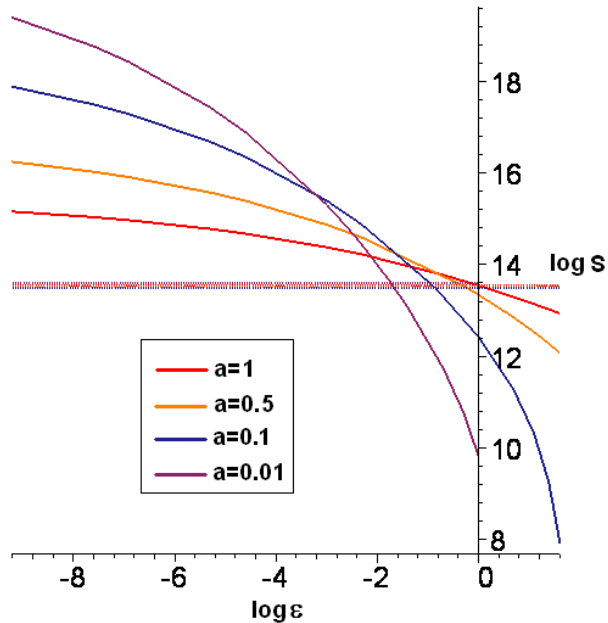


Figure 4: The Hawking-Page transition. The horizontal lines represent the values of the cascading black hole action for the four cases analyzed in this paper. The curves show the ϵ -dependence of the corresponding KS actions.

Finally, the results of the actions comparison are presented in fig.4. Curves represent the variation with ϵ of the KS action. Each curve with a given color must be compared with the horizontal line of the same color, i.e, with the cascading black hole with the corresponding temperature. As we can see, in each of these cases, the deconfined phase dominates for small values of ϵ , while the confined phase dominates for large values of this parameter. The larger the value of a , the larger the value of ϵ for the phase transition to take place.

A limitation of the approach described here is that it works for relatively small values of ϵ , implying relatively small values of a . Otherwise, the correction given by (3.39) might stop to being small. Moreover, the difference between the KS solutions with $Q = 0$ and $Q \neq 0$ could contribute as well. Our calculations indicate that the transition can be detected for values as large as $\epsilon = 10$ ($a \sim 1$).

4 Some properties of a confining field theory at finite temperature via gauge/gravity duality

4.1 The running of the gauge couplings at finite temperature

One of the most interesting properties of the cascading solutions is that they encode the running of a gauge coupling. In particular the matching of the supergravity modes with the two gauge couplings takes the form [10]:

$$\begin{aligned} \frac{4\pi^2}{g_1^2} + \frac{4\pi^2}{g_2^2} &= \frac{\pi}{g_s e^\Phi}, \\ \frac{4\pi^2}{g_1^2} - \frac{4\pi^2}{g_2^2} &= \frac{1}{g_s e^\Phi} \left[\frac{1}{2\pi\alpha'} \left(\int_{S^2} B_2 \right) - \pi \right]. \end{aligned} \quad (4.1)$$

For the KT and KS solutions one finds a result that exactly matches the field theory value of the running coupling for a gauge theory with $SU(N + M) \times SU(N)$ gauge group.

For the cascading black hole solutions we can assume that a similar correspondence holds and evaluate B_2 . The integral of B_2 over the appropriate two-cycle is proportional to the function $f(u)$ in (2.4). Since our solution is numerical we need first to find out what is the behavior of $f(u)$ in the UV regime. If we assume that as $u \rightarrow 0$,

$$f(u) \approx -\frac{B}{4} P e^{\Phi(u)} \ln(au) + f_r, \quad (4.2)$$

where f_r is a constant, then criterion (2.28) fixes

$$B = \lim_{u_{sing} \rightarrow 0} 4 \frac{e^{4(y_0+w_0)}}{\Phi_1 + \frac{1}{u_{sing}}}.$$

The pole in this expression is expected to be cancelled by the logarithmic singularity in Eq.(4.2). Substituting B in (4.2), we compare the behavior of the resulting expression with the numerical solution for $f(u)$ near u_{sing} . Denoting their difference as Δf , the obtained results are presented in figure (5) for all four cases in table 1.

It can be seen, in the UV regime, that up to corrections well below 10^{-10} , f_r is indeed a constant. The approximated values of f_r corresponding to the analyzed cases are $\{3.22186396, 2.22309019, 0.99140974, 0.41584279\}$.

Thus, the running of the difference of the inverse squares of the coupling constants have several interesting properties. First, it is proportional to P which is the parameter breaking the conformal invariance. More importantly, we have the following

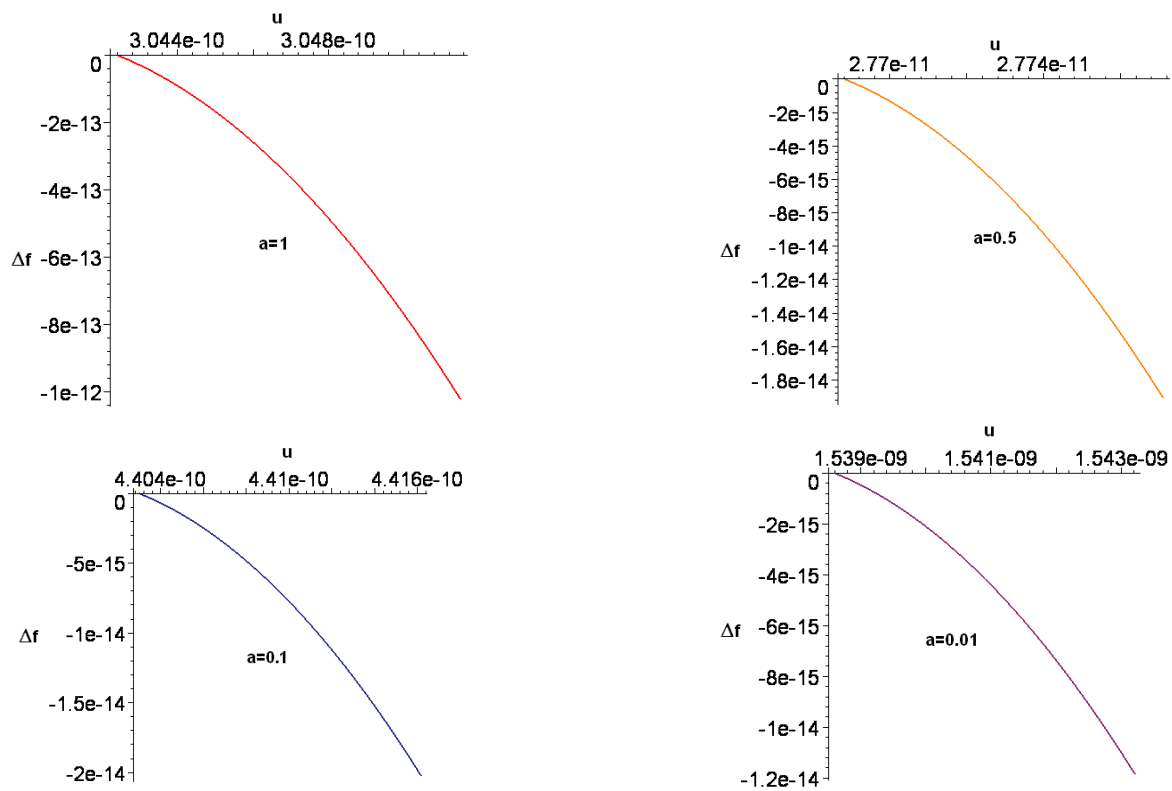


Figure 5: Behavior of Δf for $a = 1, 0.5, 0.1, 0.01$. Since it is clearly below our ‘zero’ of 10^{-10} , this shows that equation (4.2) represents very accurately the form of $f(u)$ in the UV-limit.

$$\ln(au) \sim \ln\left(\frac{\rho_0^4}{\rho^4}\right) \sim \ln\left(\frac{T}{\Lambda}\right). \quad (4.3)$$

In the above expression we have used that $2a = \rho_0^4$, where ρ_0 is the position of the horizon in the standard nonextremal D3-brane solution. Further $\rho_0 = T\pi R^2$ for nonextremal D3 branes and finally $u \approx 1/4\rho^4$ in the uv region.

Thus, we conclude that the gravity dual of the cascading black hole has

$$\frac{1}{g_1^2} - \frac{1}{g_2^2} \sim P \ln\left(\frac{\Lambda}{T}\right). \quad (4.4)$$

It is worth stressing that the high temperature behavior of the gauge coupling in Yang-Mills theories depends on the renormalization schemes at finite T . There also seem to be some discrepancies between the imaginary and real time formalism. In a sense our result should be interpreted as the string theory prediction and it coincides with the general perturbative reasoning [25, 26].

4.2 The viscosity bound

In this section we simply note that the solution [15] satisfies the condition of [27] which implies the viscosity bound. Namely, we find that for the metric (2.1) the Ricci tensor satisfies

$$R^0_0 - R^1_1 = 4e^{2z-10y} \frac{d^2x(u)}{du^2}. \quad (4.5)$$

This expression is identically zero due to the equation of motion of x .

In principle, it has been argued that the above expression is sufficient to guarantee the viscosity bound [27, 28]. We will nevertheless proceed to check the bound explicitly. The main reason being that our background is cascading and that might involve subtleties not considered in previous analysis and also that [27] used some noncovariant counterterms. Since our solutions satisfy the criterion (2.23), we obtain for the shear diffusion constant,

$$D = \frac{|\alpha - 3|}{16\pi} \frac{1}{T}.$$

Assuming the black hole temperature to be given by (2.27), for the viscosity-entropy ratio,

$$\frac{\eta}{s} = \frac{|\alpha - 3|}{16\pi}.$$

In Fig (6) we can observe that, for all the four cases in table 1, $\alpha \rightarrow -1$ from below as u approach the horizon. In this figure the values of u were conveniently rescaled for

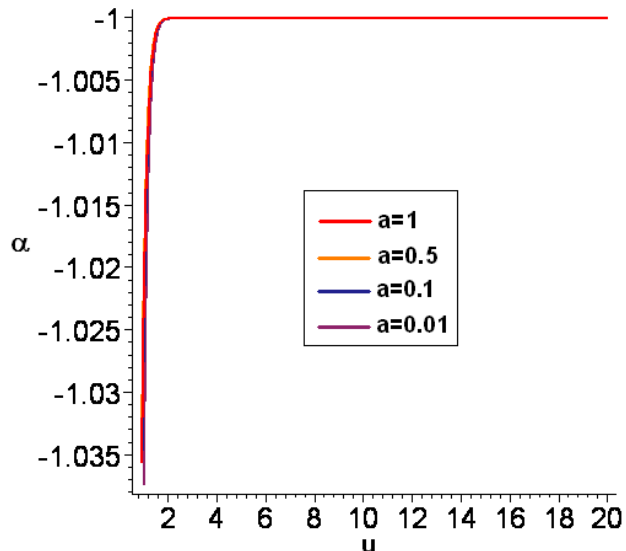


Figure 6: Behavior of the parameter α as $u \rightarrow u_{hor}$.

each case using the ratio between the different values of a . The result seems to indicate that indeed the inequality is saturated. We must note here that, in all the cases we analyzed, the value to which α converges is actually slightly bigger than -1 . For these four cases we obtained $\{-0.999999937, -0.999999946, -0.999999977, -0.999999997\}$. Nevertheless, since the difference with respect to -1 is too close to our numerical ‘zero’ we regard this effect as a numerical artifact due to the proximity to the horizon.

4.3 Drag force

In this section we apply the analysis of [32, 33] to discuss the drag force on a quark moving in a strongly coupled plasma. We emphasize the general conditions for a supergravity background to admit the motion of a classical string that can be interpreted as a drag force on a moving quark. Our analysis mirrors the generality discussed in [34], however, here we do not assume AdS asymptotics, in particular we aim at understanding cascading backgrounds.

We consider here a five-dimensional subspace of a supergravity background dual to a field theory.

$$ds^2 = -G_{00}X_0^2 + G_{xx}(dX_1^2 + dX_2^2 + dX_3^2) + G_{uu}du^2, \quad (4.6)$$

where the metric components G_{MN} are functions of the radial coordinate u only. Fol-

lowing [32, 33], we assume the world-sheet to be embedded as $t = X_0$ and $\sigma = u$ and we allow for

$$X_1 = vt + \xi(u), \quad (4.7)$$

which means that the end of the string is moving with velocity v . In the field theory side we interpret the end of the string as a quark moving with velocity v . The Nambu-Goto action is

$$S = \frac{1}{2\pi\alpha'} \int dt d\sigma \sqrt{[G_{00}(G_{uu} + G_{xx}\xi'^2) - G_{xx}G_{uu}v^2]}. \quad (4.8)$$

Since the action does not depend explicitly on σ , one has that the conjugate momenta $\frac{\partial L}{\partial \xi'}$ is a constant, where L is the Lagrangian,

$$\Pi_\xi = \frac{\partial L}{\partial \xi'} = -\frac{G_{00}G_{xx}\xi'}{\sqrt{G_{00}(G_{uu} + G_{xx}\xi'^2) - G_{uu}G_{xx}v^2}}. \quad (4.9)$$

It can be rearranged to obtain

$$\xi' = \Pi_\xi \sqrt{\frac{G_{uu}(G_{00} - G_{xx}v^2)}{G_{00}G_{xx}(G_{00}G_{xx} - \Pi_\xi^2)}}. \quad (4.10)$$

A key simplifying observation is that, since ξ' cannot be imaginary, we need both expressions in numerator and denominator to flip signs simultaneously. This fixes Π_ξ to be

$$\Pi_\xi^2 = G_{00}(x)G_{xx}(u_*). \quad (4.11)$$

Here, u_* denotes the radial coordinate satisfying

$$G_{00}(u_*) = G_{xx}(u_*)v^2. \quad (4.12)$$

The rate of change of momentum is calculated to be

$$\frac{dp_1}{dt} = \sqrt{-g}T^u{}_{x_1}, \quad (4.13)$$

where

$$T^u{}_{x_1} = -\frac{1}{2\pi\alpha'} G_{x_1\nu} g^{u\alpha} \phi_\alpha X^\nu. \quad (4.14)$$

Here, G_{ij} denotes the metric in (4.6), while g_{ij} denotes the induced metric on the world-sheet. After some algebraic simplifications, we obtain

$$\frac{dp_1}{dt} = -\frac{1}{2\pi\alpha'} \Pi_\xi. \quad (4.15)$$

We can rewrite of above equation as

$$\frac{dp_1}{dt} = -kp_1, \quad (4.16)$$

if condition (4.12) dictates Π_ξ to be proportional to p_1 . In the above equation, k is the drag force constant.

Conditions for drag force

Let us discuss the conditions under which we can observe a drag force proportional to the momentum. We need to solve for a radial position u_* such that

$$v^2 = G_{00}(u_*)/G_{xx}(u_*). \quad (4.17)$$

The expression for the canonical momentum is

$$\Pi_\xi = vG_{xx}(u_*(v)). \quad (4.18)$$

So, the question for a drag force essentially boils down to verifying that

$$G_{xx}(u_*(v)) = \frac{b}{\sqrt{1-v^2}}, \quad (4.19)$$

where b is a constant.

Two comments are in order about the relevant energy scales and the speed of the quarks:

- The nonrelativistic motion of the probe corresponding to small v is localized near the points where G_{00} vanishes. This corresponds, generically, to the horizon. In terms of energy scales, it corresponds to the infrared region.
- Relativistic velocities v close to the speed of light correspond to radial positions for which $G_{00} \approx G_{xx}$. Generically, this is the asymptotic region, which in terms of the field theory is the ultraviolet region and corresponds to the near conformal limit.

Non-extremal D3 brane

In the case of non-extremal D3 branes we have that

$$G_{00} = u^2 \left(1 - \frac{u_0^4}{u^4} \right), \quad G_{xx} = u^2. \quad (4.20)$$

The equation that determines the position u_* as a function of the velocity of the end of the string is thus:

$$v^2 = \frac{G_{00}}{G_{xx}} = \left(1 - \frac{u_0^4}{u_*^4} \right). \quad (4.21)$$

Thus, we find

$$u_*^2 = \frac{u_0^2}{\sqrt{1-v^2}}. \quad (4.22)$$

We can now easily verify that

$$G_{xx}(u_*(v)) = u_*^2 = \frac{u_0^2}{\sqrt{1-v^2}}. \quad (4.23)$$

This expression coincides with the criterion (4.19). This case was discussed in Refs.[32, 33].

Cascading black holes

Here we simply adjust the computation of the drag force presented, for example, in [32, 33]. The calculations presented here were, in particular, performed in [35, 36] without using the full metric of the cascading black hole. The AdS part of the metric in consideration in string frame is

$$ds^2 = e^{\Phi/2} [e^{2z} (-e^{-6x} dX_0^2 + e^{2x} dX_i dX^i) + e^{10y-2z} du^2] \quad (4.24)$$

We consider the worldsheet to be along $t = X_0$ and $\sigma = u$ directions. Following the general arguments at the beginning of this subsection

$$\Pi_\xi = \sqrt{v} e^{\frac{\Phi}{2} + 2z} (u(x(v))) \quad (4.25)$$

Here, u is chosen to satisfy $v = e^{-4x(u)}$ for a given v . This relation is to be viewed as an equation for the radial coordinate u , it defines a particular value u_p . We need to evaluate relation (4.25) at $u = u_p$ and, in turn, find Π_ξ as a function of v . Further, to establish the existence of a drag force we need to verify the existence of a b such that

$$\Pi_\xi = b \frac{v}{\sqrt{(1-v^2)}}, \quad (4.26)$$

which thus implies that $\Pi_\xi = \frac{b}{m} p_1$ and directly leads to a drag force parameter using equations (4.15) and (4.16). With this aim, equating equations (4.25) and (4.26) we obtain,

$$\begin{aligned} b(u) &= \sqrt{2} e^{\frac{\Phi}{2} + 2z} \sqrt{\sinh(4au)} \\ v(u) &= e^{-4au}. \end{aligned} \quad (4.27)$$

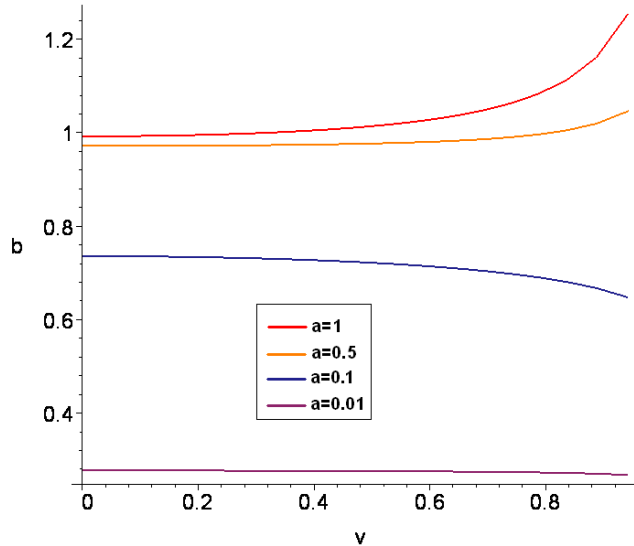


Figure 7: Behavior of the drag force parameter b as a function of the quark velocity v .

First, note that in the IR regime ($u \rightarrow \infty$),

$$b \rightarrow e^{\frac{\Phi(u)}{2}} e^{2z_*} e^{2(\alpha+1)au}, \quad (4.28)$$

where we used the asymptotical expression (2.22) for $z(u)$. In the pure D3 case, where $\Phi(u) = 0$ and $\alpha = -1$, we have that $b = \exp(2z_*)$. Recalling that, as shown in subsection 4.2, for our solution $\alpha \approx -1$, and noting that the dilaton is very weak near the horizon (for instance, for our four cases we obtained $\Phi_* \approx \{-3 \times 10^{-7}, -2 \times 10^{-7}, -1.2 \times 10^{-7}, -1.4 \times 10^{-8}\}$), we see that for the cascading black hole $b \approx \text{constant}$ in the IR-limit.

On the other hand, knowing that as $u \rightarrow 0$, $z(u)$ behaves as described by Eq.(2.29), we obtain,

$$b \rightarrow \sqrt{2ae^{\frac{\Phi_0}{2}}}, \quad (4.29)$$

implying that b is finite in the UV-limit.

This way, we have shown *analytically* that when the string explores any of the two asymptotic regions, we verify the existence of a drag force. For a given temperature the variability of b from one regime to the other is mainly related to the dilaton variability. In fig.7 we show the drag force coefficient b as given by Eqs.(4.27) for all values of v , that is, for all velocities of the external quarks. The curves represent the four cases in table 1. It is worth stressing that in the relativistic regime there is a clear velocity dependence in the coefficient b . However, for the range of values of temperatures that

we have explored it, it does not seem to be universal. In particular, the fig.7 shows that in the regime of relativistic velocities some curves have inflections upwards while other bend downward. Clearly, it seems to depend on the temperature and deserves further study.

5 Discussion and outlook

In this paper we have established numerically the existence of a Hawking-Page phase transition between the supergravity solution of [15] which represents a black hole in a cascading background and the Klebanov-Strassler solution.

We also studied some properties of the deconfined phase given by our cascading black hole solution. For instance, we have found that the difference of the inverse squares of the coupling constants is proportional to P (which is the parameter breaking the conformal invariance) and that it runs as $\ln(\Lambda/T)$.

We also verify that our solution seems to satisfy the well-known bound for the viscosity to entropy ratio.

Finally, we have explicitly shown that the universal form of the horizon in this theory guarantees the existence of a drag force for a fundamental string moving in this background and in the dual field theory that can be interpreted as jet quenching. The near horizon region describes nonrelativistic motion of the quarks and since the near horizon geometry has been shown to be universal we conclude that the nonrelativistic drag force on the quarks is also universal in the class of cascading theories. In the relativistic region we also found a well-defined drag force parameter. Numerically, we observed a velocity dependence for this parameter in the relativistic region.

It is important to stress that most of the calculations performed in this paper requires knowing the solution for all values of the radius and that an analysis solely based on the asymptotic near the horizon is not reliable.

Let us conclude with listing a number of possible directions. Cascading theories, along the lines of the particular model described here are generic in the AdS/CFT. In fact, we believe that there might be infinite classes of them based on some results presented in [37, 38]. The fact that the cone over $Y^{p,q}$ does not admit complex deformations seems like a deterrent for a construction directly mimicking the warped deformed conifold of Klebanov and Strassler but a more general solution where the fluxes play a crucial role are not ruled out. Turning on temperature for this solutions should not change substantially the asymptotic UV form obtained in [37, 38].

It would be interesting to better understand the charges in the comparison between the cascading black hole with the KS background. Basically the KS solution has $Q = 0$, that is, the number of D3 branes at the tip deformed conifold equal to zero. As shown in [9] and reviewed in section 3.2.1, we see that nonzero Q results in a singularity at the origin. Another interesting direction would be the construction of black holes in the backgrounds with back reacted flavor such [39]. In particular, some of these backgrounds should be natural generalizations of the construction of [15].

While this manuscript was in the final stage of its preparation, a new paper was posted where the authors claim to have found evidence for a transition in a solution with a black hole in the IR and KT in the UV [40]. We plan an in-depth discussion of the relation between our and their solutions. Preliminarily, let us note here that there are some key differences between our solutions. First, as far as we understand, to find their solution they need to numerically look for a zero of a function in ten variables, i.e., the norm of their 'mismatch vector'. Since this is a positive semi-definite function, assuming that this zero exists, this problem can be translated into finding the global minimum of a 10D-surface. Nevertheless, this is a case of constrained optimization, since the Hamiltonian constrain is also valid in ten dimensions, where it shows as a reparametrization of the radial coordinate. However, the authors of [40] made no mention to whether their solution satisfies this constrain. As oppose to that, our solutions are forced to automatically satisfy the zero-energy constrain and that this certainly happen is one of the main criteria of quality we use to certify our numerical output. This was first explained in Ref. [15] and emphasized in this manuscript. Secondly, their solution seems to have exactly KT in the boundary (we note here that the KT solution does not satisfy the Hamiltonian constrain for $a \neq 0$) and to erase the large u singularity typical of KT (we called this singular point as u_{sing}), pasting the black hole metric in the IR solution somewhere in the 'middle' of the radial domain. Our solution extents from u_{sing} to infinity and, as explained in Section 2.4, we set $u_{sing} = 0$ to guarantee the completeness of our background.

Acknowledgments

We thank Alex Buchel for various comments, Elena Cáceres for comments on the drag force and Javier Mas for various useful comments and explanations about related matters. This work is partially supported by Department of Energy under grant DE-FG02-95ER40899 to the University of Michigan and by grant CNPq/CLAF-150548/2004-4.

C. T-E thanks the MCTP for hospitality during the final stages of this work and LPZ thanks Universidad de Santiago de Compostela for a very warm hospitality.

References

- [1] J. M. Maldacena, “The large N limit of superconformal field theories and supergravity,” *Adv. Theor. Math. Phys.* **2** (1998) 231 [*Int. J. Theor. Phys.* **38** (1999) 1113] [arXiv:hep-th/9711200].
- [2] O. Aharony, S. S. Gubser, J. M. Maldacena, H. Ooguri and Y. Oz, “Large N field theories, string theory and gravity,” *Phys. Rept.* **323** (2000) 183 [arXiv:hep-th/9905111].
- [3] S. S. Gubser, I. R. Klebanov and A. W. Peet, “Entropy and Temperature of Black 3-Branes,” *Phys. Rev. D* **54** (1996) 3915 [arXiv:hep-th/9602135].
I. R. Klebanov and A. A. Tseytlin, “Entropy of Near-Extremal Black p-branes,” *Nucl. Phys. B* **475** (1996) 164 [arXiv:hep-th/9604089]. S. S. Gubser, I. R. Klebanov and A. A. Tseytlin, “Coupling constant dependence in the thermodynamics of N = 4 supersymmetric Yang-Mills theory,” *Nucl. Phys. B* **534** (1998) 202 [arXiv:hep-th/9805156].
- [4] E. Witten, “Anti-de Sitter space, thermal phase transition, and confinement in gauge theories,” *Adv. Theor. Math. Phys.* **2** (1998) 505 [arXiv:hep-th/9803131].
- [5] I. R. Klebanov and E. Witten, “Superconformal field theory on threebranes at a Calabi-Yau singularity,” *Nucl. Phys. B* **536** (1998) 199 [arXiv:hep-th/9807080].
- [6] S. S. Gubser and I. R. Klebanov, “Baryons and domain walls in an N = 1 superconformal gauge theory,” *Phys. Rev. D* **58** (1998) 125025 [arXiv:hep-th/9808075].
- [7] I. R. Klebanov and N. A. Nekrasov, “Gravity duals of fractional branes and logarithmic RG flow,” *Nucl. Phys. B* **574** (2000) 263 [arXiv:hep-th/9911096].
- [8] I. R. Klebanov and A. A. Tseytlin, “Gravity duals of supersymmetric SU(N) x SU(N+M) gauge theories,” *Nucl. Phys. B* **578** (2000) 123 [arXiv:hep-th/0002159].
- [9] I. R. Klebanov and M. J. Strassler, “Supergravity and a confining gauge theory: Duality cascades and chiSB-resolution of naked singularities,” *JHEP* **0008** (2000) 052 [arXiv:hep-th/0007191].

- [10] C. P. Herzog, I. R. Klebanov and P. Ouyang, “D-branes on the conifold and $N = 1$ gauge / gravity dualities,” arXiv:hep-th/0205100.
- [11] A. Buchel, “Finite temperature resolution of the Klebanov-Tseytlin singularity,” Nucl. Phys. B **600** (2001) 219 [arXiv:hep-th/0011146].
- [12] A. Buchel, C. P. Herzog, I. R. Klebanov, L. A. Pando Zayas and A. A. Tseytlin, “Non-extremal gravity duals for fractional D3-branes on the conifold,” JHEP **0104** (2001) 033 [arXiv:hep-th/0102105].
- [13] S. S. Gubser, C. P. Herzog, I. R. Klebanov and A. A. Tseytlin, “Restoration of chiral symmetry: A supergravity perspective,” JHEP **0105** (2001) 028 [arXiv:hep-th/0102172].
- [14] O. Aharony, A. Buchel and A. Yarom, “Holographic renormalization of cascading gauge theories,” Phys. Rev. D **72** (2005) 066003 [arXiv:hep-th/0506002].
- [15] L. A. Pando Zayas and C. A. Terrero-Escalante, JHEP **0609** (2006) 051 [arXiv:hep-th/0605170].
- [16] D. Marolf, “Chern-Simons terms and the three notions of charge,” arXiv:hep-th/0006117.
- [17] A. Buchel, “Transport properties of cascading gauge theories,” Phys. Rev. D **72** (2005) 106002 [arXiv:hep-th/0509083].
- [18] L. A. Pando Zayas and A. A. Tseytlin, “3-branes on resolved conifold,” JHEP **0011** (2000) 028 [arXiv:hep-th/0010088].
- [19] O. Aharony, J. Sonnenschein and S. Yankielowicz, “A holographic model of deconfinement and chiral symmetry restoration,” arXiv:hep-th/0604161.
- [20] D. Mateos, R. C. Myers and R. M. Thomson, “Holographic phase transitions with fundamental matter,” arXiv:hep-th/0605046.
- [21] P. Benincasa and A. Buchel, “Hydrodynamics of Sakai-Sugimoto model in the quenched approximation,” arXiv:hep-th/0605076.
- [22] A. Parnachev and D. A. Sahakyan, “Chiral phase transition from string theory,” arXiv:hep-th/0604173.

- [23] T. Albash, V. Filev, C. V. Johnson and A. Kundu, “A topology-changing phase transition and the dynamics of flavour,” arXiv:hep-th/0605088.
- [24] L. A. Pando Zayas, *Confinement/Deconfinement Transition in AdS / CFT* ,
[http://www.perimeterinstitute.ca/en/Events/
Exotic_States_of_Hot_and_Dense_Matter_and_their_Dual_Description/View_Lectures/](http://www.perimeterinstitute.ca/en/Events/Exotic_States_of_Hot_and_Dense_Matter_and_their_Dual_Description/View_Lectures/)
- [25] J. I. Kapusta and C. Gale, *Finite-Temperature Field Theory Principles and Applications*, Cambridge University Press, 2006.
- [26] M. Bellac, *Thermal Field Theory*, Cambridge University Press, 1996.
- [27] A. Buchel, *Phys. Lett. B* **609** (2005) 392 [arXiv:hep-th/0408095].
- [28] A. Buchel and J. T. Liu, *Phys. Rev. Lett.* **93** (2004) 090602 [arXiv:hep-th/0311175].
- [29] C. P. Herzog, *Phys. Rev. Lett.* **98** (2007) 091601 [arXiv:hep-th/0608151].
- [30] C. A. Ballon Bayona, H. Boschi-Filho, N. R. F. Braga and L. A. Pando Zayas, arXiv:0705.1529 [hep-th].
- [31] I. R. Klebanov and A. Murugan, *JHEP* **0703** (2007) 042 [arXiv:hep-th/0701064].
- [32] C. P. Herzog, A. Karch, P. Kovtun, C. Kozcaz and L. G. Yaffe, *JHEP* **0607** (2006) 013 [arXiv:hep-th/0605158].
- [33] S. S. Gubser, *Phys. Rev. D* **74** (2006) 126005 [arXiv:hep-th/0605182].
- [34] C. P. Herzog, *JHEP* **0609** (2006) 032 [arXiv:hep-th/0605191].
- [35] A. Buchel, *Phys. Rev. D* **74** (2006) 046006 [arXiv:hep-th/0605178].
- [36] E. Caceres and A. Guijosa, *JHEP* **0612** (2006) 068 [arXiv:hep-th/0606134].
- [37] C. P. Herzog, Q. J. Ejaz and I. R. Klebanov, *JHEP* **0502** (2005) 009 [arXiv:hep-th/0412193].
- [38] B. A. Burrington, J. T. Liu, M. Mahato and L. A. Pando Zayas, *JHEP* **0507** (2005) 019 [arXiv:hep-th/0504155].

- [39] F. Benini, F. Canoura, S. Cremonesi, C. Nunez and A. V. Ramallo, arXiv:0706.1238 [hep-th].
F. Benini, F. Canoura, S. Cremonesi, C. Nunez and A. V. Ramallo, JHEP **0702** (2007) 090 [arXiv:hep-th/0612118].
- [40] O. Aharony, A. Buchel and P. Kerner, arXiv:0706.1768 [hep-th].